Optimizing Interface Conductivity in Electronics

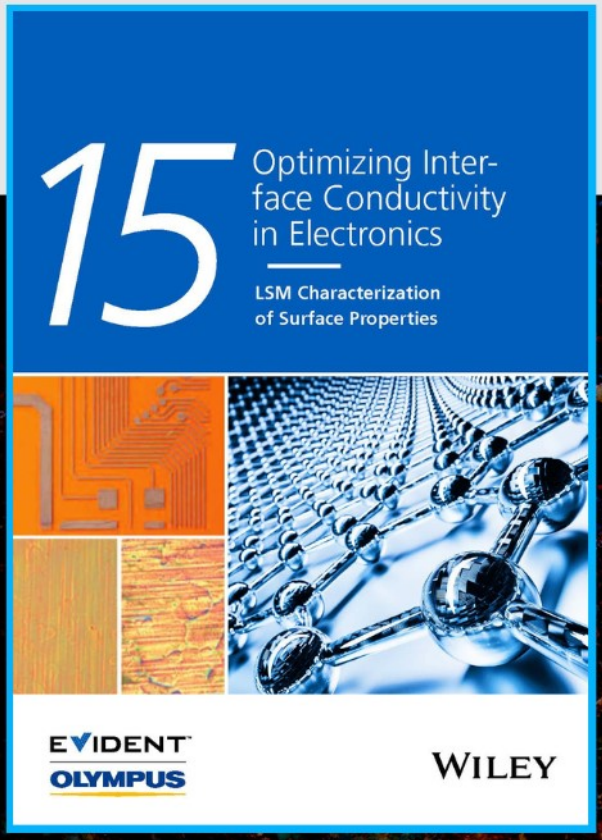

The latest eBook from Advanced Optical Metrology. Download for free.

Surface roughness is a key parameter for judging the performance of a given material's surface quality for its electronic application. A powerful tool to measure surface roughness is 3D laser scanning confocal microscopy (LSM), which will allow you to assess roughness and compare production and finishing methods, and improve these methods based on mathematical models.

Focus on creating high-conductivity electronic devices with minimal power loss using laser scanning microscopy is an effective tool to discern a variety of roughness parameters.

EVIDENT
OLYMPUS

WILEY

Received: 26 October 2022 | Revised: 11 March 2023 | Accepted: 16 April 2023

DOI: 10.1002/rnc.6738

RESEARCH ARTICLE

WILEY

Observer-based memory-event-triggered controller design for quarter-vehicle suspension systems subject to deception attacks

Xiang Sun | **Zhou Gu** | **Xiufeng Mu**

College of Mechanical & Electronic Engineering, Nanjing Forestry University, Nanjing, China

Correspondence
Zhou Gu, College of Mechanical & Electronic Engineering, Nanjing forestry University, Nanjing 210037, China.
Email: gzh1808@163.com

Funding information
National Natural Science Foundation of China, Grant/Award Numbers: 62273183, 62022044, 62103193; Postgraduate Research & Practice Innovation Program of Jiangsu Province, Grant/Award Number: KYCX20_0855

Abstract

This paper concerns the problem of an observer-based memory-event-triggered controller for quarter-vehicle suspension systems (SSs) under deception attacks. The observer-based controller is utilized to solve the difficulty that full state information of quarter-vehicle SSs cannot be obtained. A memory-event-triggered mechanism (METM) considering both network load and observer performance is proposed, where the historical information of the measured output is utilized in the event-triggered condition and the observer, reducing mal-triggering events caused by abrupt disturbance and enhancing the sensitivity to deception attacks. Sufficient conditions that guarantees an H_∞ performance of quarter-vehicle SSs are presented. Finally, a simulation example under the bump road conditions is provided to validate the effectiveness of the derived controller.

KEYWORDS

deception attacks, memory event-triggered mechanism, observer-based controller, quarter-vehicle suspension systems

1 | INTRODUCTION

Nowadays, networked suspension systems (SSs) have been introduced to improve the performance requirements of ride comfort, road holding, and suspension deflection.[1-6] Networked SSs, such as cloud-aided SSs in Reference 7, can offer more incredible benefits in forecasting, optimizing,[8] and cooperative driving strategy than conventional SSs. Furthermore, networked SS is more cost-effective since it needs fewer sophisticated technological devices per vehicle and utilizes modern communications technology to provide enough computation and data storage capacity. However, most previous work generally requires that full states of SSs are available, which is a challenging problem in most practical measurements of SSs due to the constraints of sensors. Therefore, observer-based control (see References 9-12) as an effective method has been widely concerned in controller design, especially in SSs. in Reference 13, the proposed Takagi–Sugeno (T–S) fuzzy controller based on disturbance observer only needs the information of easily measured seat acceleration and suspension deflection variables. Considering that full states information of SSs is unavailable, the authors in Reference 14 proposed a new observer-based H_∞ controller for active SSs to improve the ride comfort of passengers and save the network bandwidth. In Reference 15, to solve the problem of the unmeasured current state variable in SSs with magnetorheological damper, an observer-based sliding mode control approach was put forward.

Abbreviations: ETM, event-triggered mechanism; METM, memory-event-triggered mechanism; SS, suspension system; T–S, Takagi–Sugeno.

For networked SSs, the time-triggered data transmission strategy has advantages in analysis and design, but it will occupy a lot of network bandwidth and communication resources. To reduce the burden of communication networks, the event-triggered mechanism (ETM) has appeared in recent years, by which the sampled packets are transmitted over the network only when the preset triggering condition is violated.[16-23] However, how to choose reasonable triggering conditions which can cope with different situations has become a new problem, wherefore, some state-of-art ETMs have been put forward. For example, two novel dynamic ETMs are proposed in Reference 24 to coordinate the transmission of sampled data so that data transmission can be scheduled in a way that saves more network bandwidth. in Reference 25, an adaptive ETM was proposed for nonlinear discrete-time systems, which considers an auxiliary dynamic variable when designing event-triggered conditions. The threshold design of adaptive ETM in Reference 26 depends on the system states. Under this ETM, the event-triggered conditions can be adjusted with the dynamic states of the nonlinear networked interconnected control system. In addition, the authors also considered the adaptive event triggering conditions for interconnected control systems with stochastic uncertainty in Reference 27. To achieve better performance of the power systems under random deception attacks, a METM was presented in Reference 28, wherein historical triggered information was utilized in the proposed event triggering condition. Therefore, designing reasonable triggering conditions that can save the limited network bandwidth and guarantee the desired performance has become a hot topic.

It should be noted that the data information is transmitted via wireless networks in the framework of networked SSs. Due to the openness of wireless networks,[29-31] the secure control for networked SSs under cyber attacks becomes a complicated and challenging problem. Among modes of cyber attacks, deception attack is a common mode, by which adversaries randomly replace the transmitted data with false data when it is transmitted over the network.[28,32-36] The event-triggered filtering problem of the fuzzy-model-based cyber-physical systems under deception attacks was studied in Reference 37, where the proposed event-triggered filter that generates data-releasing events based on the present sampling data and the most recent releasing data can ensure the filter security. In Reference 38, the author addressed the challenge of distributed recursive filter design for time-delayed stochastic systems subject to deception attacks. In addition, the network-induced delay[39-43] in networked SSs data transmission cannot be ignored. However, little attention has been involved to observer-based event-triggered controller design for networked SSs under deception attacks, which motivates this study.

Inspired by the anterior discussion, we will solve the problem of observer-based memory-event-triggered controller design for quarter-vehicle SSs subject to deception attacks in this paper. The major contributions can be summarized as follows.

(1) The previous releasing information of the measured output is introduced into the event-triggered mechanism to reduce the amount of mal-triggering events caused by abrupt disturbance and the data releasing rate. In addition, a cross term between error and measured output is considered in the event-triggered mechanism, resulting in better control performance due to the sensitivity of the proposed ETM to deception attacks.
(2) A memory-event-triggered observer utilizing historical information is constructed to address the absence of full state information, leading to better observer performance and control performance of quarter-vehicle SSs.

The remainder of this paper is summarized in what follows. The problem formulation and main results are introduced in Sections 2 and 3, respectively. Section 4 illustrates the effectiveness of proposed observer-based memory-event-triggered controller by simulation examples. The conclusion and future research direction are drawn in Section 5.

1.1 | Notations

We define the following notations in this paper. $\mathbf{He}\{X\}$ represents the sum of X and X^T; diag$\{\ldots\}$ stands for a diagonal matrix; $\mathcal{E}\{*\}$ denotes the expectation of $\{*\}$.

2 | PROBLEM FORMULATION

Similar to Reference 4, the model of the active quarter-vehicle SS in Figure 1 which can be represented as:

$$\begin{cases} \dot{x}(t) = Ax(t) + Bu(t) + D\omega(t) \\ y(t) = Cx(t) \end{cases}, \tag{1}$$

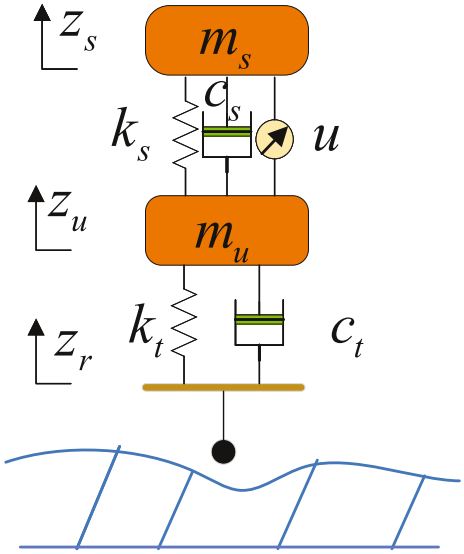

FIGURE 1 Quarter-vehicle suspension system.

where

$$A = \begin{bmatrix} 0 & 0 & 1 & -1 \\ 0 & 0 & 0 & 1 \\ -\frac{k_s}{m_s} & 0 & -\frac{c_s}{m_s} & \frac{c_s}{m_s} \\ \frac{k_s}{m_u} & -\frac{k_t}{m_u} & \frac{c_s}{m_u} & -\frac{c_s+c_t}{m_u} \end{bmatrix}, \quad B = \begin{bmatrix} 0 & 0 & \frac{1}{m_s} & -\frac{1}{m_u} \end{bmatrix}^T,$$
$$C = \begin{bmatrix} 1 & 0 & 0 & 0 \end{bmatrix}, \quad D = \begin{bmatrix} 0 & -1 & 0 & \frac{c_t}{m_u} \end{bmatrix}^T.$$

and the symbols of k_s, k_t, c_s, c_t, m_s, and m_u can be found in Reference 44.

Before designing observer-based memory-event-triggered controller, we first review the general observer-based controller for the quarter-vehicle SS, which can be expressed as:

$$\begin{cases} \dot{\hat{x}}(t) = A\hat{x}(t) + Bu(t) + L[y(t) - \hat{y}(t)] \\ \hat{y}(t) = C\hat{x}(t), \\ u(t) = K\hat{x}(t), \end{cases} \tag{2}$$

where L and K are the gains of the observer and controller that need to be designed, respectively.

As is shown in Figure 2, output signal $y(t)$ of the SS collected by sensor is transmitted to the observer through wireless network. To save the network bandwidth and ensure the performance of the quarter-vehicle SS subject to deception attacks, a memory-event-triggered observer with queue buffer is put forward. The periodic sampled output $y(i_k h)$ (h is sampling period and i_k denotes the kth sampling sequence) that can be released to the observer is determined by the following memory-event-triggered condition:

$$t_{k+1}h = t_k h + \min\{vh \mid \psi(t) > 0\}, \tag{3}$$

with

$$\psi(t) = \sum_{m=1}^{3} \nu_m e_m^T(t)\Omega e_m(t) - \ell(t) > 0,$$

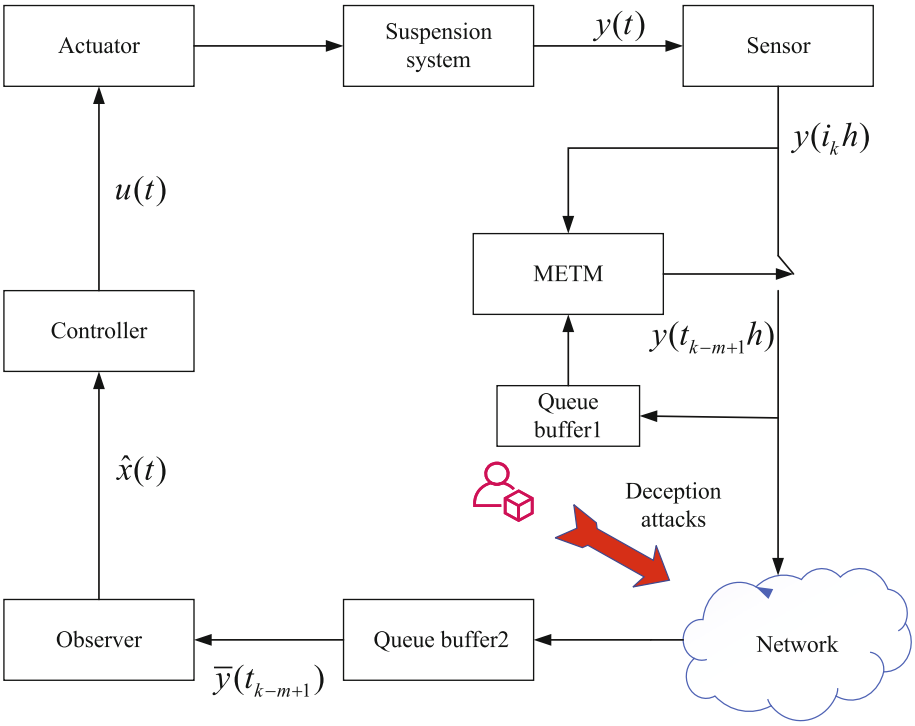

FIGURE 2 The frame structure of the observer-based memory-event-triggered quarter-vehicle suspension system.

where

$$e_m(t) = \check{y}_m(t) - y(t_k h + vh), \check{y}_m(t) = \frac{y(t_{k-m+1}h) + y(t_k h + vh)}{2}$$
$$\ell(t) = \sigma_1 \ell_1^T(t)\Omega\ell_1(t) + \frac{\sigma_2}{2}\left[\ell_1^T(t)\Omega\ell_2(t) + \ell_2^T(t)\Omega\ell_1(t)\right],$$
$$\ell_1(t) = \frac{1}{3}\sum_{m=1}^{3} y(t_{k-m+1}h), \ell_2(t) = \sum_{m=1}^{3} \nu_m e_m(t), m = 1, 2, \ldots .$$

Remark 1. m released data packets are introduced to be the input of the ETM, and the error $\check{y}_m(t)$ is a mean value of the released data packet $y(t_{k-m+1}h)$ and current sampling packet $y(t_k h + vh)$, by which mal-triggering events caused by abrupt disturbance can be reduced, such as a gross measuring error.

Remark 2. The introduction of more historical packets into ETM input requires more storage space and more computing resources, therefore, we use three historical triggering data to realize the advantages mentioned above, that is $\overline{m}$ (the maximum of m) is set to be 3. When $\overline{m} = 1$, the METM turns into a general ETM. To simplify the expression, the following parts of this paper use $m \in \{1, 2, 3\}$.

Remark 3. Different from traditional observer in (2), the memory-event-triggered observer we proposed uses historical measured output information as input to solve the problem of the absence of full state information for quarter-vehicle SSs, which can get better observer performance and control performance.

Remark 4. To make the proposed event-triggering condition more sensitive to deception attacks, we introduce a new item $\frac{\sigma_2}{2}[\ell_1^T(t)\Omega\ell_2(t) + \ell_2^T(t)\Omega\ell_1(t)]$ in (3), by which the data releasing rate increases during the occurrence of deception attacks, thereby enhancing the performance of SSs.

As is seen in Figure 2, wireless communication network is vulnerable to cyber attacks. The adversaries inject attack signal $g_m(y(t_{k-m+1}h))$ into the output $y(t_{k-m+1}h)$. It leads to

$$\bar{y}(t_{k-m+1}h) = \alpha(t)g_m(y(t_{k-m+1}h)) + (1 - \alpha(t))y(t_{k-m+1}h), \quad (4)$$

where $\alpha(t) \in \{0,1\}$ is a Bernoulli random variable with $\mathcal{E}\{\alpha(t)\} = \overline{\alpha}$, $\mathcal{E}\{(\alpha(t)-\overline{\alpha})^2\} = \overline{\alpha}(1-\overline{\alpha}) = \hat{\alpha}^2$, and $\alpha(t)$ being 1 represents deception attacks are successfully injected on the transmission signal.

Remark 5. To avoid being detected, the deception attack function $g_m(y(t))$ is assumed to satisfy the following condition:

$$\|g_m(y(t))\|_2 \leq \|Gy(t)\|_2, \tag{5}$$

where G is a constant matrix.

Combing memory-event-triggered condition (3) and the actual input of observer (4), we can obtain the memory-event-triggered observer as follows

$$\dot{\hat{x}}(t) = A\hat{x}(t) + Bu(t) + \sum_{m=1}^{3} L_m[\bar{y}(t_{k-m+1}h) - \hat{y}(t)]. \tag{6}$$

Define η_k as the network-induced delay of the released packet at $t_k h$. Assume the upper bound of η_k is $\overline{\eta}$. Due to the queue buffer 2, we know that $[t_k h + \eta_k, t_{k+1}h + \eta_{k+1}) = \bigcup_{v=0}^{v_M} \Upsilon_{t_k}^v$ with $\Upsilon_{t_k}^v = [t_k h + vh + \eta_k^v, t_{k+1}h + vh + h + \eta_{k+1}^{v+1})$.

Similar to Reference 16, we define

$$\eta(t) = t - t_k h - vh, \quad t \in \Upsilon_{t_k}^v, \tag{7}$$

where $0 \leq \eta(t) \leq h + \overline{\eta} = \eta_M$.

From memory-event-triggered condition (3) and (7), one has

$$y(t_{k-m+1}h) = y(t - \eta(t)) + 2e_m(t). \tag{8}$$

Combine (3), (4), and (8), the memory-event-triggered observer in (6) can be represented as

$$\begin{aligned}\dot{\hat{x}}(t) = \sum_{m=1}^{\overline{m}} \big[&A\hat{x}(t) + Bu(t) + \alpha(t)L_m g_m(y(t_{k-m+1}h)) + (1-\alpha(t))L_m Cx(t-\eta(t)) \\ &+ (1-\alpha(t))2L_m e_m(t) - L_m C\hat{x}(t)\big].\end{aligned} \tag{9}$$

Similar to the traditional observer-based controller in (2), the control input can be designed as

$$u(t) = K\hat{x}(t). \tag{10}$$

Next, defining the observer estimation error $\tilde{e}(t) = x(t) - \hat{x}(t)$ yields that

$$\begin{cases}\dot{\hat{x}}(t) = \sum_{m=1}^{\overline{m}} \big[(A + BK - L_m C)\hat{x}(t) + (1-\alpha(t))L_m C\tilde{e}(t-\eta(t)) + (1-\alpha(t))L_m C\hat{x}(t-\eta(t)) \\ \qquad + (1-\alpha(t))2L_m e_m(t) + \alpha(t)L_m g_m(y(t_{k-m+1}h))\big], \\ \dot{\tilde{e}}(t) = \sum_{m=1}^{\overline{m}} \big[A\tilde{e}(t) - (1-\alpha(t))L_m C\tilde{e}(t-\eta(t)) - (1-\alpha(t))L_m C\hat{x}(t-\eta(t)) + L_m C\hat{x}(t) \\ \qquad - (1-\alpha(t))2L_m e_m(t) + D\omega(t) - \alpha(t)L_m g_m(y(t_{k-m+1}h))\big].\end{cases} \tag{11}$$

Define $\zeta^T(t) = \begin{bmatrix}\hat{x}^T(t) & \tilde{e}^T(t)\end{bmatrix}$. By utilizing equations in (11), the observer-based memory-event-triggered SS can be expressed as

$$\begin{aligned}\dot{\zeta}(t) = \sum_{m=1}^{\overline{m}} [&\mathcal{A}_m\zeta(t) + (1-\alpha(t))\mathcal{B}_{1m}\zeta(t-\eta(t)) + (1-\alpha(t))2\mathcal{B}_{2m}e_m(t) \\ &+ \alpha(t)\mathcal{B}_{2m}g_m(y(t_{k-m+1}h)) + \mathcal{D}\omega(t)\big],\end{aligned} \tag{12}$$

where

$$\mathcal{A}_m = \begin{bmatrix} A+BK-L_mC & 0 \\ L_mC & A \end{bmatrix}, \quad \mathcal{B}_{1m} = \begin{bmatrix} L_mC & L_mC \\ -L_mC & -L_mC \end{bmatrix}, \quad \mathcal{B}_{2m} = \begin{bmatrix} L_m \\ -L_m \end{bmatrix}, \quad \mathcal{D} = \begin{bmatrix} 0 \\ D \end{bmatrix}.$$

Based on the above discussion, in this paper, we aim to design a novel memory observer-based event-triggered controller for the networked quarter-vehicle SS subject to deception attacks.

3 | MAIN RESULTS

Theorem 1. *For given positive parameters $\eta_M, \sigma_1 \in [0,1), \sigma_2 \in [0,1), \overline{\alpha}, \hat{\alpha}, \gamma$ and $\nu_m \in [0,1), m \in \{1,2,3\}$, and matrices K, L_m, G. The memory observer-based event-triggered SS (12) is asymptotically stable in the mean square sense, if there exist symmetric positive matrices $P, Q, R, \overline{X}_1, \Omega$ and matrices U such that the following inequalities hold*:

$$\Pi = \begin{bmatrix} \Theta_{11} & * & * & * \\ \Theta_{21} & \Theta_{22} & * & * \\ \Theta_{31} & 0 & \Theta_{33} & * \\ \Theta_{41} & \Theta_{42} & \Theta_{43} & \Theta_{44} \end{bmatrix} < 0, \tag{13}$$

$$\tilde{R} = \begin{bmatrix} R & * \\ U & R \end{bmatrix} > 0, \tag{14}$$

where

$$\Theta_{11} = \begin{bmatrix} \Xi_1 & * & * \\ \Xi_2 & -2R+U+U^T+\Xi_3 & * \\ U^T & R^T-U^T & -Q-R \end{bmatrix}, \quad \Theta_{21} = \begin{bmatrix} \Xi_{e1}P & \mu_{11}\Omega C\mathcal{I} & 0 \\ \Xi_{e2}P & \mu_{12}\Omega C\mathcal{I} & 0 \\ \Xi_{e3}P & \mu_{13}\Omega C\mathcal{I} & 0 \end{bmatrix},$$

$$\Theta_{22} = \begin{bmatrix} \mu_{21}\Omega & * & * \\ \mu_3\Omega & \mu_{22}\Omega & * \\ \mu_4\Omega & \mu_5\Omega & \mu_{23}\Omega \end{bmatrix}, \quad \Theta_{31} = \begin{bmatrix} \Xi_{g1}P & 0 & 0 \\ \Xi_{g2}P & 0 & 0 \\ \Xi_{g3}P & 0 & 0 \\ \mathcal{D}^TP & 0 & 0 \end{bmatrix}, \quad \Theta_{41} = \begin{bmatrix} \eta_M\sum_{m=1}^3 \mathcal{A}_m & \eta_M(1-\overline{\alpha})\sum_{m=1}^3 \mathcal{B}_{1m} & 0 \\ 0 & \eta_M\hat{\alpha}\sum_{m=1}^3 \mathcal{B}_{1m} & 0 \\ C\mathcal{I} & 0 & 0 \\ \sqrt{3}GC\mathcal{I} & 0 & 0 \end{bmatrix},$$

$$\Theta_{42} = \begin{bmatrix} \eta_M\Xi_{e1}^T & \eta_M\Xi_{e2}^T & \eta_M\Xi_{e3}^T \\ 2\eta_M\hat{\alpha}\mathcal{B}_{21} & 2\eta_M\hat{\alpha}\mathcal{B}_{22} & 2\eta_M\hat{\alpha}\mathcal{B}_{23} \\ 0 & 0 & 0 \\ 0 & 0 & 0 \end{bmatrix}, \quad \Theta_{43} = \begin{bmatrix} \eta_M\Xi_{g1}^T & \eta_M\Xi_{g2}^T & \eta_M\Xi_{g3}^T & \eta_M\mathcal{D} \\ \eta_M\hat{\alpha}\mathcal{B}_{21} & \eta_M\hat{\alpha}\mathcal{B}_{22} & \eta_M\hat{\alpha}\mathcal{B}_{23} & 0 \\ 0 & 0 & 0 & 0 \\ 0 & 0 & 0 & 0 \end{bmatrix},$$

$$\Theta_{33} = \{-\overline{X}_1^{-1}, -\overline{X}_1^{-1}, -\overline{X}_1^{-1}, -\gamma^2 I\}, \quad \Theta_{44} = \{-R^{-1}, -R^{-1}, -I, -\overline{X}_1\},$$

$$\Xi_1 = \sum_{m=1}^3 \{P\mathcal{A}_m + \mathcal{A}_m^TP + Q - R\}, \quad \Xi_2 = (1-\overline{\alpha})\sum_{m=1}^3 (\mathcal{B}_{1m}^TP) + R^T - U^T,$$

$$\Xi_3 = \sigma_1\mathcal{I}^TC^T\Omega C\mathcal{I}, \mathcal{I} = \begin{bmatrix} I_p & I_p \end{bmatrix}, \quad \Xi_{em} = 2(1-\overline{\alpha})\mathcal{B}_{2m}^T, \quad \Xi_{gm} = \overline{\alpha}\mathcal{B}_{2m}^T,$$

$$\mu_{1m} = \frac{2}{3}\sigma_1 + \frac{1}{2}\sigma_2\nu_m, \quad \mu_{2m} = \frac{4}{9}\sigma_1 + \frac{2}{3}\sigma_2\nu_m - \nu_m, \quad \mu_3 = \frac{4}{9}\sigma_1 + \frac{1}{3}\sigma_2\nu_1 + \frac{1}{3}\sigma_2\nu_2,$$

$$\mu_4 = \frac{4}{9}\sigma_1 + \frac{1}{3}\sigma_2\nu_1 + \frac{1}{3}\sigma_2\nu_3, \quad \mu_5 = \frac{4}{9}\sigma_1 + \frac{1}{3}\sigma_2\nu_2 + \frac{1}{3}\sigma_2\nu_3.$$

Proof. Construct the following Lyapunov functional for the system (12):

$$V(t) = \zeta^T(t)P\zeta(t) + \int_{t-\eta_M}^{t} \zeta^T(s)Q\zeta(s)ds + \eta_M \int_{t-\eta_M}^{t}\int_{s}^{t} \dot{\zeta}^T(v)R\dot{\zeta}(v)dvds, \tag{15}$$

where $P = \text{diag}\{P_1, P_1\} > 0$.

Then, we have

$$\begin{aligned}\mathcal{E}\left\{\dot{V}(t)\right\} = \mathcal{E}\Big\{ & 2\zeta^T(t)P\dot{\zeta}(t) + \zeta^T(t)Q\zeta(t) - \zeta^T(t-\eta_M)Q\zeta(t-\eta_M) \\ & + \eta_M^2\dot{\zeta}^t(t)R\dot{\zeta}(t) - \eta_M\int_{t-\eta_M}^{t}\dot{\zeta}^T(s)R\dot{\zeta}(s)ds\Big\}.\end{aligned} \tag{16}$$

To facilitate expression, we define $\xi(t) = [\zeta^T(t)\ \ \zeta^T(t-\eta(t))\ \ \zeta^T(t-\eta_M)\ \ \vartheta_e^T(t)\ \ \vartheta_g^T(t)\ \ \omega^T(t)]^T$, where $\vartheta_e(t) = [e_1^T(t)\ \ e_2^T(t)\ \ e_3^T(t)]^T$, $\vartheta_g(t) = [g_1^T(y(t))\ \ g_2^T(y(t))\ \ g_3^T(y(t))]^T$.

Note that

$$\mathcal{E}\left\{\dot{\zeta}^T(t)R\dot{\zeta}(t)\right\} = \xi^T(t)(\mathcal{H}_1^T R\mathcal{H}_1 + \mathcal{H}_2^T R\mathcal{H}_2)\xi(t), \tag{17}$$

where

$$\begin{aligned}\mathcal{H}_1 &= \left[\mathcal{A}\quad (1-\overline{\alpha})\textstyle\sum_{m=1}^{3}\mathcal{B}_{1m}\quad 0\quad 2(1-\overline{\alpha})\mathcal{F}\quad \overline{\alpha}\mathcal{F}\quad \mathcal{D}\right], \\ \mathcal{H}_2 &= \left[0\quad \hat{\alpha}\textstyle\sum_{m=1}^{3}\mathcal{B}_{1m}\quad 0\quad 2\hat{\alpha}\mathcal{F}\quad \hat{\alpha}\mathcal{F}\quad 0\right],\quad \mathcal{F} = \left[\mathcal{B}_{21}\quad \mathcal{B}_{22}\quad \mathcal{B}_{23}\right].\end{aligned}$$

Next, it can be easily obtained

$$\begin{aligned}&-\eta_M\int_{t-\eta_M}^{t}\dot{\zeta}^T(s)R\dot{\zeta}(s)ds \\ &= -\eta_M\int_{t-\eta(t)}^{t}\dot{\zeta}^T(s)R\dot{\zeta}(s)ds - \eta_M\int_{t-\eta_M}^{t-\eta(t)}\dot{\zeta}^T(s)R\dot{\zeta}(s)ds.\end{aligned} \tag{18}$$

Applying Jensen's inequality, one can obtain

$$\begin{aligned}&-\eta_M\int_{t-\eta(t)}^{t}\dot{\zeta}^T(s)R\dot{\zeta}(s)ds \\ &\le -\frac{\eta_M}{\eta(t)}\left(\int_{t-\eta(t)}^{t}\dot{\zeta}^T(s)ds\right)R\left(\int_{t-\eta(t)}^{t}\dot{\zeta}(s)ds\right).\end{aligned} \tag{19}$$

and

$$\begin{aligned}&-\eta_M\int_{t-\eta_M}^{t-\eta(t)}\dot{\zeta}^T(s)R\dot{\zeta}(s)ds \\ &\le -\frac{\eta_M}{\eta_M-\eta(t)}\left(\int_{t-\eta_M}^{t-\eta(t)}\dot{\zeta}^T(s)ds\right)R\left(\int_{t-\eta_M}^{t-\eta(t)}\dot{\zeta}(s)ds\right).\end{aligned} \tag{20}$$

From (19) and (20), the following inequality can be further deduced by

$$\begin{aligned}-\eta_M\int_{t-\eta_M}^{t}\dot{\zeta}^T(s)R\dot{\zeta}(s)ds &\le \chi^T(t)\mathcal{R}\chi(t), \\ \chi(t) &= [\zeta^T(t)\ \ \zeta^T(t-\eta(t))\ \ \zeta^T(t-\eta_M)]^T,\end{aligned} \tag{21}$$

$$\mathcal{R}=\begin{bmatrix} -R & * & * \\ R^T-U^T & -2R^T+U+U^T & * \\ U^T & R^T-U^T & -R \end{bmatrix}.$$

Compared with some existing event-triggered controller design approaches, the methods of Jensen inequality with free-weighting-matrix were used in deriving the criteria of observer-based memory-event-triggered controller design for quarter-vehicle systems to reduce the conservativeness.

From the inequality in (5), it yields that

$$g_m^T(y(t))\overline{X}_1^{-1}g_m(y(t))-y^T(t)G^T\overline{X}_1^{-1}Gy(t)\le 0, \tag{22}$$

where $\overline{X}_1$ is a symmetric positive matrix.

Taking the derivation and expectation to $V(t)$, combining (15)–(22) and METM in (3), then using Schur complement yield that

$$\mathcal{E}\left\{\dot{V}(t)-\gamma^2\omega^T(t)\omega(t)+y^T(t)y(t)\right\}\le\xi^T(t)\Pi\xi(t),$$

From (13), it has $\mathcal{E}\left\{\dot{V}(t)\right\}<0$. That is to say, the observer-based memory-event-triggered system (12) is asymptotically stable in the mean square sense. The proof is completed. ∎

Sufficient conditions that guarantee the mean square asymptotic stability of the system (12) are achieved in Theorem 1. Next, we will present the design method of the memory-event-triggered observer gain and controller gain of SS against deception attacks.

Theorem 2. *For given positive parameters $\eta_M, \sigma_1\in[0,1), \sigma_2\in[0,1), \overline{\alpha}, \hat{\alpha}, \gamma$ and $\nu_m\in[0,1), m\in\{1,2,3\}$. The observer memory-based event-triggered SS (12) is asymptotically stable in the mean square sense, if there exist positive constant ε and symmetric positive matrices $X, \hat{Q}, \hat{R}, \hat{\Omega}, \overline{X}_1$, and matrices $\hat{U}, Y_1, T_m, m\in\{1,2,3\}$, such that the following inequalities hold*:

$$\hat{\Pi}=\begin{bmatrix} \hat{\Theta}_{11} & * & * & * \\ \hat{\Theta}_{21} & \hat{\Theta}_{22} & * & * \\ \hat{\Theta}_{31} & 0 & \hat{\Theta}_{33} & * \\ \hat{\Theta}_{41} & \hat{\Theta}_{42} & \hat{\Theta}_{43} & \hat{\Theta}_{44} \end{bmatrix}<0, \tag{23}$$

$$\hat{\mathcal{R}}=\begin{bmatrix} \hat{R}_1 & * & * & * \\ 0 & \hat{R}_2 & * & * \\ \hat{U}_1^T & 0 & \hat{R}_1 & * \\ 0 & \hat{U}_2^T & 0 & \hat{R}_2 \end{bmatrix}>0, \tag{24}$$

$$\mathcal{M}=\begin{bmatrix} -\epsilon I & * \\ \overline{X}_1C-CX_1 & -I \end{bmatrix}<0, \tag{25}$$

where

$$\hat{\Theta}_{11}=\begin{bmatrix} \hat{\Xi}_1 & * & * \\ \hat{\Xi}_2 & -2\hat{R}+\hat{U}+\hat{U}^T+\hat{\Xi}_3 & * \\ \hat{U}^T & \hat{R}^T-\hat{U}^T & -\hat{Q}-\hat{R} \end{bmatrix},\quad \hat{\Theta}_{21}=\begin{bmatrix} \hat{\Xi}_{e1} & \mu_{11}\hat{\Omega}C\mathcal{I} & 0 \\ \hat{\Xi}_{e2} & \mu_{12}\hat{\Omega}C\mathcal{I} & 0 \\ \hat{\Xi}_{e3} & \mu_{13}\hat{\Omega}C\mathcal{I} & 0 \end{bmatrix},$$

$$\hat{\Theta}_{22}=\begin{bmatrix} \mu_{21}\hat{\Omega} & * & * \\ \mu_3\hat{\Omega} & \mu_{22}\hat{\Omega} & * \\ \mu_4\hat{\Omega} & \mu_5\hat{\Omega} & \mu_{23}\hat{\Omega} \end{bmatrix},\quad \hat{\Theta}_{31}=\begin{bmatrix} \hat{\Xi}_{g1} & 0 & 0 \\ \hat{\Xi}_{g2} & 0 & 0 \\ \hat{\Xi}_{g3} & 0 & 0 \\ \mathcal{D}^T & 0 & 0 \end{bmatrix},\quad \hat{\Theta}_{41}=\begin{bmatrix} \eta_M\hat{\Xi}_4 & \eta_M(1-\overline{\alpha})\tilde{\Xi}_2^T & 0 \\ 0 & \eta_M\hat{\alpha}\hat{\Xi}_2^T & 0 \\ \hat{\Xi}_5 & 0 & 0 \\ \hat{\Xi}_6 & 0 & 0 \end{bmatrix},$$

$$\hat{\Theta}_{42}=\begin{bmatrix}\eta_M\hat{\Xi}_{e1}^T & \eta_M\hat{\Xi}_{e2}^T & \eta_M\hat{\Xi}_{e3}^T\\ 2\eta_M\hat{\alpha}\hat{T}_1^T & 2\eta_M\hat{\alpha}\hat{T}_2^T & 2\eta_M\hat{\alpha}\hat{T}_3^T\\ 0 & 0 & 0\\ 0 & 0 & 0\end{bmatrix},\quad \hat{\Theta}_{43}=\begin{bmatrix}\eta_M\hat{\Xi}_{g1}^T & \eta_M\hat{\Xi}_{g2}^T & \eta_M\hat{\Xi}_{g3}^T & \eta_M D\\ \eta_M\hat{\alpha}\hat{T}_1^T & \eta_M\hat{\alpha}\hat{T}_2^T & \eta_M\hat{\alpha}\hat{T}_3^T & 0\\ 0 & 0 & 0 & 0\\ 0 & 0 & 0 & 0\end{bmatrix},$$

$$\hat{\Theta}_{33}=\{-\overline{X}_1,-\overline{X}_1,-\overline{X}_1,-\gamma^2 I\},\quad \hat{\Theta}_{44}=\{\varepsilon^2\hat{R}-2\varepsilon X,\varepsilon^2\hat{R}-2\varepsilon X,-I,-\overline{X}_1\}.$$

$$\hat{\Xi}_1=\begin{bmatrix}\hat{\Xi}_{11} & *\\ \sum_{m=1}^{3}(T_mC) & \hat{\Xi}_{12}\end{bmatrix}+\hat{Q}-\hat{R},\quad \tilde{\Xi}_2=\begin{bmatrix}\hat{\Xi}_{21} & -\hat{\Xi}_{21}\\ \hat{\Xi}_{21} & -\hat{\Xi}_{21}\end{bmatrix},$$

$$\hat{\Xi}_2=(1-\overline{\alpha})\tilde{\Xi}_2+\hat{R}^T-\hat{U}^T,\quad \hat{\Xi}_3=\sigma_1\mathcal{I}^TC^T\hat{\Omega}C\mathcal{I},$$

$$\hat{\Xi}_4=\begin{bmatrix}AX_1+BY_1-\sum_{m=1}^{3}(T_mC) & 0\\ \sum_{m=1}^{3}(T_mC) & AX_1\end{bmatrix},$$

$$\hat{\Xi}_5=\begin{bmatrix}\overline{X}_1C & \overline{X}_1C\end{bmatrix},\quad \hat{\Xi}_6=\begin{bmatrix}\sqrt{3}G\overline{X}_1C & \sqrt{3}G\overline{X}_1C\end{bmatrix},$$

$$\hat{\Xi}_{11}=\boldsymbol{He}\{AX_1+BY_1-\sum_{m=1}^{3}(T_mC)\},\quad \hat{\Xi}_{12}=\boldsymbol{He}\{AX_1\},$$

$$\hat{\Xi}_{21}=\sum_{m=1}^{3}(C^TT_m^T),\quad \hat{\Xi}_{em}=2(1-\overline{\alpha})\hat{T}_m,\quad \hat{\Xi}_{gm}=\overline{\alpha}\hat{T}_m,\quad \hat{T}_m=[T_m^T\quad -T_m^T].$$

Furthermore, the controller and memory-based observer gain can be obtained as follows:

$$K=Y_1X_1^{-1},\quad L_m=T_m\overline{X}_1^{-1}. \tag{26}$$

Proof. Define $Y_1=KX_1$, $CX_1=\overline{X}_1C$, $T_m=L_m\overline{X}_1$, $\hat{Q}_1=X_1Q_1X_1$, $\hat{Q}_2=X_1Q_2X_1$, $\hat{Q}=\text{diag}\{\hat{Q}_1,\hat{Q}_2\}$, $\hat{R}_1=X_1R_1X_1$, $\hat{R}_2=X_1R_2X_1$, $\hat{R}=\text{diag}\{\hat{R}_1,\hat{R}_2\}$, $\hat{U}_1=X_1U_1X_1$, $\hat{U}_2=X_1U_2X_1$, $\hat{U}=\text{diag}\{\hat{U}_1,\hat{U}_2\}$, $\hat{\Omega}=\overline{X}_1\Omega\overline{X}_1$.

Let $X=\text{diag}\{X_1,X_1\}$, $X_1=P_1^{-1}$, $\mathcal{X}=\text{diag}\{X,X,X,\underbrace{\overline{X}_1,\cdots,\overline{X}_1}_{6},\underbrace{I,\cdots,I}_{7}\}$, then pre- and postmultiply Π with $\mathcal{X}$ and $\mathcal{X}^T$. Combining $-PR^{-1}P\le-2\varepsilon P+\varepsilon^2R$ and the optimization algorithm in Reference 45, one can conclude that (23), (24), and (25) can ensure $\mathcal{E}\{\dot{V}(t)\}<0$. This ends the proof. ∎

Remark 6. Note that the METM in (3) will degrade to the conventional ETM in Reference 16 when choosing $\overline{m}=1$ and $\sigma_2=0$. Then the following corollary is achieved for the observer-based event-triggered SS.

Corollary 1. *For given positive parameters η_M, $\sigma_1\in[0,1)$, $\overline{\alpha}$, $\hat{\alpha}$, and γ. The observer-based event-triggered SS (12) is asymptotically stable in the mean square sense, if there exist positive constant ε and symmetric positive matrices X, $\hat{Q}$, $\hat{R}$, $\hat{\Omega}$ and matrices $\hat{U}$, Y_1, T, $\overline{X}_1$, such that*

$$\hat{\Pi}=\begin{bmatrix}\hat{\Theta}_{11} & * & * & *\\ \hat{\Theta}_{21} & \hat{\Theta}_{22} & * & *\\ \hat{\Theta}_{31} & 0 & \hat{\Theta}_{33} & *\\ \hat{\Theta}_{41} & \hat{\Theta}_{42} & \hat{\Theta}_{43} & \hat{\Theta}_{44}\end{bmatrix}<0, \tag{27}$$

$$\hat{\mathcal{R}}=\begin{bmatrix}\hat{R}_1 & * & * & *\\ 0 & \hat{R}_2 & * & *\\ \hat{U}_1^T & 0 & \hat{R}_1 & *\\ 0 & \hat{U}_2^T & 0 & \hat{R}_2\end{bmatrix}>0, \tag{28}$$

$$\mathcal{M}=\begin{bmatrix}-\epsilon I & *\\ \overline{X}_1C-CX_1 & -I\end{bmatrix}<0, \tag{29}$$

where

$$\hat{\Theta}_{11}=\begin{bmatrix}\hat{\Xi}_1 & * & *\\ \hat{\Xi}_2 & -2\hat{R}+\hat{U}+\hat{U}^T+\hat{\Xi}_3 & *\\ \hat{U}^T & \hat{R}^T-\hat{U}^T & -\hat{Q}-\hat{R}\end{bmatrix},$$

$$\hat{\Theta}_{21}=\begin{bmatrix}\hat{\Xi}_e & \sigma_1\hat{\Omega}C\mathcal{I} & 0\end{bmatrix},\quad \hat{\Theta}_{22}=\sigma_1\hat{\Omega}-\hat{\Omega},$$

$$\hat{\Theta}_{31}=\begin{bmatrix}\hat{\Xi}_g & 0 & 0\\ D^T & 0 & 0\end{bmatrix},\quad \hat{\Theta}_{33}=\{-\overline{X}_1,-\gamma^2 I\},$$

$$\hat{\Theta}_{41}=\begin{bmatrix}\eta_M\hat{\Xi}_4 & \eta_M(1-\overline{\alpha})\hat{\Xi}_2^T & 0\\ 0 & \eta_M\hat{\alpha}\hat{\Xi}_2^T & 0\\ \hat{\Xi}_5 & 0 & 0\\ \hat{\Xi}_6 & 0 & 0\end{bmatrix},\quad \hat{\Theta}_{42}=\begin{bmatrix}\eta_M\hat{\Xi}_e^T\\ \eta_M\hat{\alpha}\hat{T}^T\\ 0\\ 0\end{bmatrix},\quad \hat{\Theta}_{43}=\begin{bmatrix}\eta_M\hat{\Xi}_g^T & \eta_M D\\ \eta_M\hat{\alpha}\hat{T}^T & 0\\ 0 & 0\\ 0 & 0\end{bmatrix},$$

$$\hat{\Theta}_{44}=\{\varepsilon^2\hat{R}-2\varepsilon X,\varepsilon^2\hat{R}-2\varepsilon X,-I,-\overline{X}_1\},$$

$$\hat{\Xi}_1=\begin{bmatrix}\hat{\Xi}_{11} & *\\ TC & \hat{\Xi}_{12}\end{bmatrix}+\hat{Q}-\hat{R},\quad \tilde{\Xi}_2=\begin{bmatrix}\hat{\Xi}_{21} & -\hat{\Xi}_{21}\\ \hat{\Xi}_{21} & -\hat{\Xi}_{21}\end{bmatrix},$$

$$\hat{\Xi}_2=(1-\overline{\alpha})\tilde{\Xi}_2+\hat{R}^T-\hat{U}^T,\quad \hat{\Xi}_3=\sigma_1\mathcal{I}^TC^T\hat{\Omega}C\mathcal{I},$$

$$\hat{\Xi}_4=\begin{bmatrix}AX_1+BY_1-TC & 0\\ TC & AX_1\end{bmatrix},$$

$$\hat{\Xi}_5=\begin{bmatrix}\overline{X}_1C & \overline{X}_1C\end{bmatrix},\hat{\Xi}_6=\begin{bmatrix}G\overline{X}_1C & G\overline{X}_1C\end{bmatrix},$$

$$\hat{\Xi}_{11}=\boldsymbol{He}\{AX_1+BY_1-TC\},\quad \hat{\Xi}_{12}=\boldsymbol{He}\{AX_1\},$$

$$\hat{\Xi}_{21}=C^TT^T,\quad \hat{\Xi}_e=(1-\overline{\alpha})\hat{T},\quad \hat{\Xi}_g=\overline{\alpha}\hat{T},\quad \hat{T}=[T^T\quad -T^T].$$

Furthermore, the controller and observer gain can be obtained in what follows

$$K=Y_1X_1^{-1},L=T\overline{X}_1^{-1}. \tag{30}$$

4 | SIMULATION EXAMPLES

To demonstrate the superiority of the proposed memory observer-based event-triggered control method, a model of the quarter-vehicle SS with the parameters in Reference 45 is carried out in this section. The road disturbance of single bump in Reference 45 is selected as

$$z_r(t)=\begin{cases}\frac{A}{2}\left(1-cos\left(\frac{2\pi V_0}{l}t\right)\right), & 0\le t\le\frac{l}{V_0}\\ 0, & t>\frac{l}{V_0}\end{cases}, \tag{31}$$

where $A=0.06\,\mathrm{m}, l=5\,\mathrm{m}, V_0=45\,\mathrm{km/h}$.

Select $h=0.01, \eta_M=0.01, \varepsilon=0.1, \epsilon=0.0085, \nu_1=0.5, \nu_2=0.3, \nu_3=0.2, \sigma_1=0.005, \overline{\alpha}=0.1, \hat{\alpha}=0.3, \gamma=4, G=0.5$, and $g(y(t))=\tanh(0.5y(t))$.

The following two cases will be studied to validate the effectiveness of our proposed method.

Case (i): The quarter-vehicle SS uses the proposed observer-based memory-event-triggered controller in (2) with $m=3$ and $\sigma_2=0.01$. Applying Theorem 2, one can derive that the weight matrix $\Omega=2.2107\times10^4$, the controller gain and observer gains are:

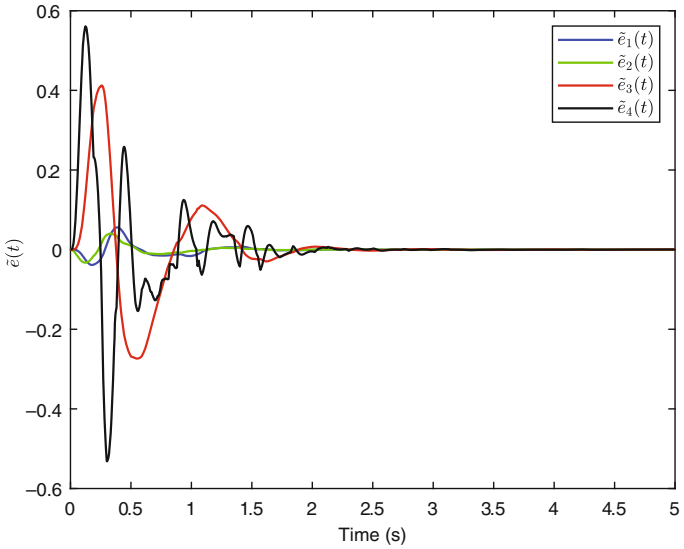

FIGURE 3 Trajectories of the observer error $\tilde{e}(t)$ in case (i).

$$K = 10^3 \times \begin{bmatrix} -5.9060 & 1.1632 & -6.7700 & 7.1741 \end{bmatrix},$$
$$L1 = \begin{bmatrix} 0.3788 & 4.2860 & 16.2937 & -138.2427 \end{bmatrix},$$
$$L2 = \begin{bmatrix} 0.1482 & 2.7341 & 10.5773 & -89.9225 \end{bmatrix},$$
$$L3 = \begin{bmatrix} 0.0238 & 1.8937 & 7.4142 & -63.1315 \end{bmatrix}.$$

Case (ii): The observer-based event-triggered quarter-vehicle SS that uses general ETM was proposed in Reference 16 with $\overline{m} = 1$ and $\sigma_2 = 0$. By utilizing Corollary 1, one can obtain

$$K = 10^4 \times \begin{bmatrix} -0.6458 & 0.0940 & -1.3840 & 1.4578 \end{bmatrix},$$
$$L = \begin{bmatrix} 0.0627 & 0.8899 & 8.2249 & -70.0916 \end{bmatrix}, \quad \Omega = 160.8781.$$

The simulation results of cases (i) and (ii) are exhibited as follows. Figures 3 and 4 illustrate the trajectories of the observer error $\tilde{e}(t)$ in cases (i) and (ii), respectively, where $\tilde{e}_i(t) = x_i(t) - \hat{x}_i(t), i = 1, 2, 3, 4$. Compared to the observer using the general ETM, we can conclude that the SS under the memory-event-triggered observer achieves better observer performance. Similar to Reference 4, the indicators of body acceleration, suspension deflection and tyre deflection under case (i), case (ii), and passive SS are plotted by red solid lines, blue solid lines, and black rash lines in Figures 5–7, respectively, from which the memory-event-triggered controller we proposed has better control performance under deception attacks and road disturbances of a single bump than the observer-based event-triggered controller using general ETM.

Figures 8 and 9 show the release intervals in cases (i) and (ii), respectively. For a clearer explanation, the average data releasing rate (ADRR) of two cases in different periods are shown in Table 1, where ADRR is denoted by ADRR $= \frac{\text{number of packet releasing (NPR)}}{\text{number of data sampling (NDS)}}$.

From Table 1, we can obtain that the ADRR during 0–2 s of the SS with an observer-based memory-event-triggered controller is higher than the one with the observer-based event-triggered controller that uses general ETM, which implies that the system with the memory-event-triggered observer receives more data to obtain better observer performance when the system suffers deception attacks and single bump disturbance, to this end, the system control performance is also guaranteed. Besides, the ADRR of 3.5–5 s in cases (i) and (ii) are 2.6% and 8.0%, respectively. Therefore, we can conclude that the proposed METM can save more network bandwidth of the SS than the general ETM when the system tends to be stable.

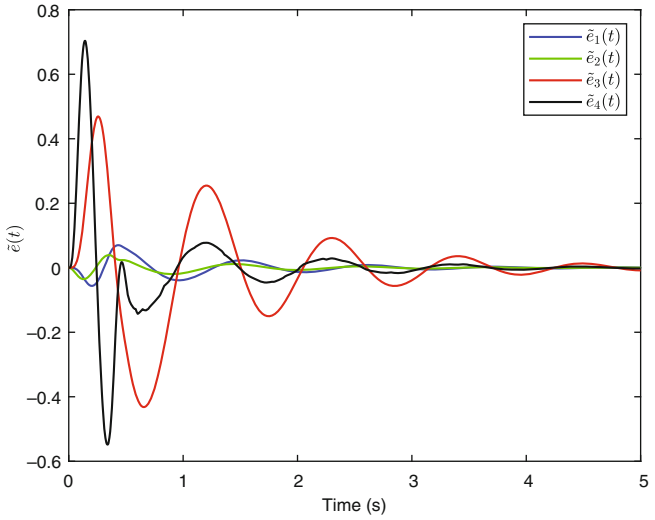

FIGURE 4 Trajectories of the observer error $\tilde{e}(t)$ in case (ii).

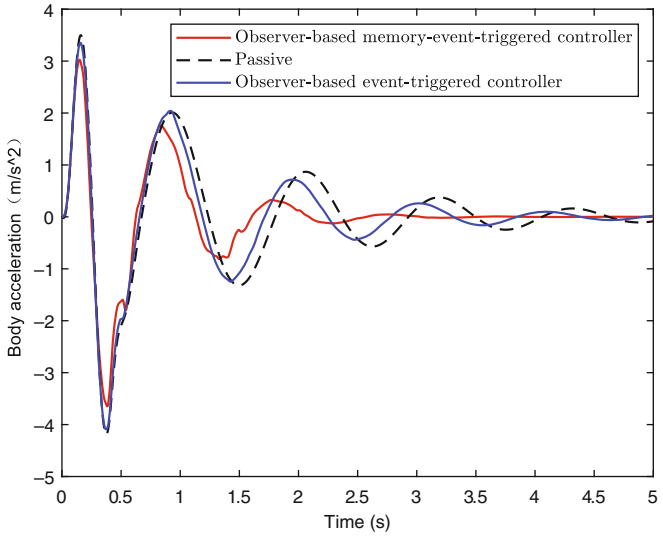

FIGURE 5 Body acceleration.

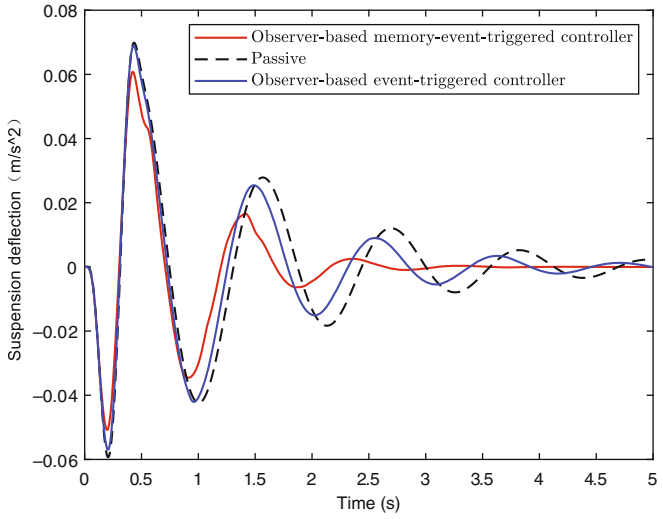

FIGURE 6 Suspension deflection.

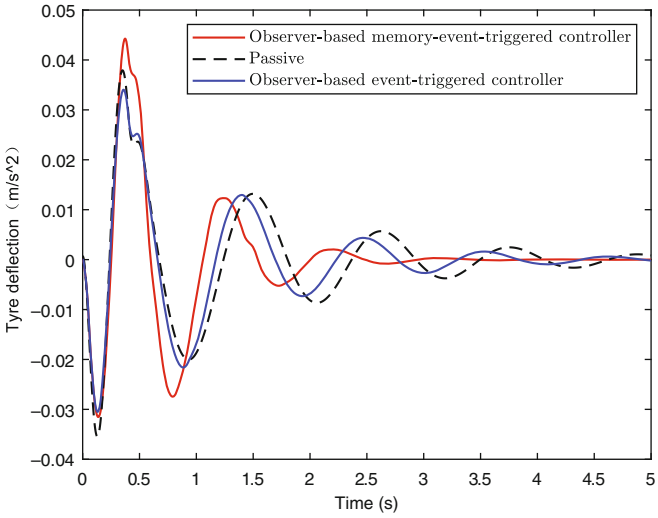

FIGURE 7 Tyre deflection.

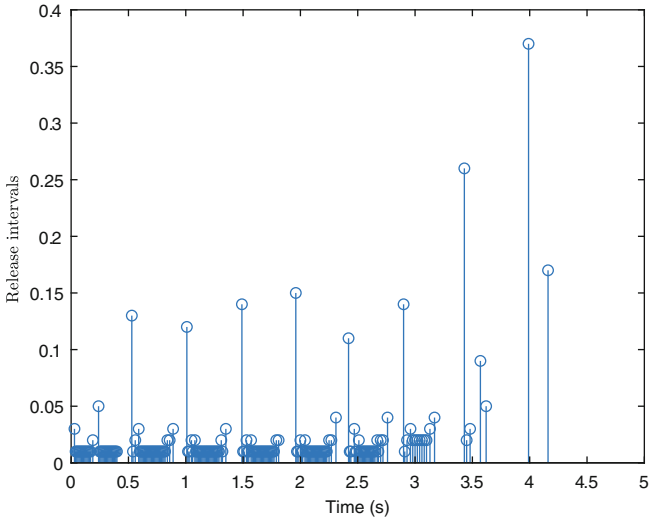

FIGURE 8 Release intervals of memory-event-triggered mechanism in case (i).

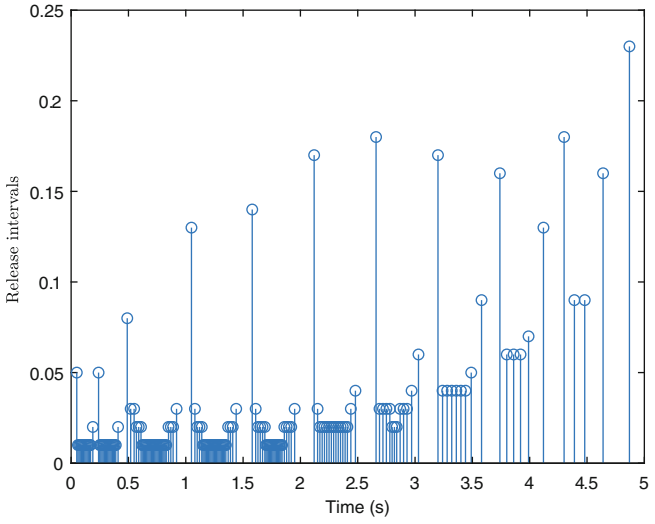

FIGURE 9 Release intervals of event-triggered mechanism in case (ii).

TABLE 1 Average data releasing rate in different periods.

Time (s)	0–2	3.5–5	0–5
METM	64.5%	2.6%	39.8%
ETM	60.0%	8.0%	34.4%

Abbreviations: ETM, event-triggered mechanism; METM, memory-event-triggered mechanism.

5 | CONCLUSIONS

The problem of memory observer-based event-triggered controller design for quarter-vehicle SSs subject to deception attacks is investigated in this paper. Considering the unavailability SSs states and the security of the communication network, a memory observer-based event-triggered control method is put forward. The performance of the quarter-vehicle SSs under deception attacks is then guaranteed. Moreover, using the historical measured output information in METM can reduce the mal-releasing packets caused by road disturbances and save considerable network bandwidth. Simulation results are given to demonstrate the effectiveness of the proposed observer-based memory-event-triggered controller. The proposed observer-based memory-event-triggered controller design method presents several challenging issues that require further investigation. These include: (i) extending the method for fault-tolerant control of SSs with actuator faults; and (ii) extending the method for interconnected event-triggered full-vehicle SSs.

ACKNOWLEDGMENTS

This work was supported in part by the National Natural Science Foundation of China under Grant 62273183, Grant 62022044, and Grant 62103193 and in part by the Postgraduate Research & Practice Innovation Program of Jiangsu Province under Grant KYCX20_0855.

CONFLICT OF INTEREST

The authors declare no potential conflict of interests.

DATA AVAILABILITY STATEMENT

Data sharing not applicable since the article describes theoretical research.

ORCID

Xiang Sun https://orcid.org/0000-0002-8951-5427
Zhou Gu https://orcid.org/0000-0002-0342-1658

REFERENCES

1. Wen S, Chen M, Zeng Z, Yu X, Huang T. Fuzzy control for uncertain vehicle active suspension systems via dynamic sliding-mode approach. *IEEE Trans Syst Man Cybern Syst*. 2017;47(1):24-32.
2. Meng Q, Qian C, Liu R. Dual-rate sampled-data stabilization for active suspension system of electric vehicle. *Int J Robust Nonlinear Control*. 2018;28(5):1610-1623.
3. Zheng X, Hao Z, Yan H, Yang F, Vlacic L. Active full-vehicle suspension control via cloud-aided adaptive backstepping approach. *IEEE Trans Cybernet*. 2019;50(7):3113-3124.
4. Li H, Zhang Z, Yan H, Xie X. Adaptive event-triggered fuzzy control for uncertain active suspension systems. *IEEE Trans Cybernet*. 2019;49(12):4388-4397.
5. Fei Z, Wang X, Liu M, Lu J, Filev D, Yu J. Reliable control for vehicle active suspension systems under event-triggered scheme with frequency range limitation. *IEEE Trans Syst Man Cybern Syst*. 2021;51(3):1630-1641.
6. Viadero-Monasterio F, Boada BL, Boada M, Diaz V. H_∞ dynamic output feedback control for a networked control active suspension system under actuator faults. *Mech Syst Signal Process*. 2022;162:108050.
7. Zhang H, Zheng X, Yan H, Peng C, Wang Z, Chen Q. Co-design of event-triggered and distributed H_∞ filtering for active semi-vehicle suspension systems. *IEEE/ASME Trans Mech*. 2017;22(2):1047-1058.
8. Zhao J, Yang C, Gao W, Zhou L. Reinforcement learning and optimal control of PMSM speed servo system. *IEEE Trans Ind Electron*. 2023;70(8):8305-8313. doi:10.1109/TIE.2022.3220886
9. Peng C, Yue D, Tian E, Gu Z. Observer-based fault detection for networked control systems with network quality of services. *Appl Math Model*. 2010;34(6):1653-1661.

10. Xie X, Yue D, Zhang H, Xue Y. Fault estimation observer design for discrete-time Takagi-Sugeno fuzzy systems based on homogenous polynomially parameter-dependent Lyapunov functions. *IEEE Trans Cybern*. 2017;47(9):2504-2513.
11. Hu S, Yue D, Han Q-L, Xie X, Chen X, Dou C. Observer-based event-triggered control for networked linear systems subject to denial-of-service attacks. *IEEE Trans Cybern*. 2020;50(5):1952-1964.
12. Qiu J, Sun K, Wang T, Gao H. Observer-based fuzzy adaptive event-triggered control for pure-feedback nonlinear systems with prescribed performance. *IEEE Trans Fuzzy Syst*. 2019;27(11):2152-2162.
13. Ning D, Sun S, Zhang F, Du H, Li W. Disturbance observer based Takagi–Sugeno fuzzy control for an active seat suspension. *Mech Syst Signal Process*. 2017;93:515-530.
14. Zhang H, Zheng X, Li H, Wang Z, Yan H. Active suspension system control with decentralized event-triggered scheme. *IEEE Trans Ind Electron*. 2020;67(12):10798-10808.
15. Chen K-Y. A new state observer-based vibration control for a suspension system with magnetorheological damper. *Vehic Syst Dyn*. 2021;60(9):3127-3150.
16. Yue D, Tian E, Han Q-L. A delay system method for designing event-triggered controllers of networked control systems. *IEEE Trans Autom Control*. 2013;58(2):475-481.
17. Yan S, Shen M, Nguang S, Zhang G. Event-triggered H_∞ control of networked control systems with distributed transmission delay. *IEEE Trans Autom Control*. 2020;65(10):4295-4301.
18. Ge X, Han Q-L, Zhang X-M, Ding L, Yang F. Distributed event-triggered estimation over sensor networks: a survey. *IEEE Trans Cybern*. 2020;50(3):1306-1320.
19. Guo X-G, Fan X, Wang J-L, Park JH. Event-triggered switching-type fault detection and isolation for fuzzy control systems under DoS attacks. *IEEE Trans Fuzzy Syst*. 2021;29(11):3401-3414.
20. Liu Y, Yang Z, Zhou H. Periodic self-triggered intermittent control with impulse for synchronization of hybrid delayed multi-links systems. *IEEE Trans Netw Sci Eng*. 2022;9(6):4087-4100.
21. Peng C, Li J, Fei M. Resilient event-triggering H_∞ load frequency control for multi-area power systems with energy-limited DoS attacks. *IEEE Trans Power Syst*. 2017;32(5):4110-4118.
22. Zong G, Ren H. Guaranteed cost finite-time control for semi-Markov jump systems with event-triggered scheme and quantization input. *Int J Robust Nonlinear Control*. 2019;29(15):5251-5273.
23. Zhang X, Han Q-L. Event-triggered H_∞ control for a class of nonlinear networked control systems using novel integral inequalities. *Int J Robust Nonlinear Control*. 2017;27(4):679-700.
24. Ge X, Ahmad I, Han Q-L, Wang J, Zhang X-M. Dynamic event-triggered scheduling and control for vehicle active suspension over controller area network. *Mech Syst Signal Process*. 2021;152:107481.
25. Hu S, Yue D, Yin X, Xie X, Ma Y. Adaptive event-triggered control for nonlinear discrete-time systems. *Int J Robust Nonlinear Control*. 2016;26(18):4104-4125.
26. Gu Z, Yue D, Tian E. On designing of an adaptive event-triggered communication scheme for nonlinear networked interconnected control systems. *Inform Sci*. 2018;422:257-270.
27. Gu Z, Shi P, Yue D. An adaptive event-triggering scheme for networked interconnected control system with stochastic uncertainty. *Int J Robust Nonlinear Control*. 2017;27(2):236-251.
28. Tian E, Peng C. Memory-based event-triggering H_∞ load frequency control for power systems under deception attacks. *IEEE Trans Cybern*. 2020;50(11):4610-4618.
29. Peng C, Sun H, Yang M, Wang Y. A survey on security communication and control for smart grids under malicious cyber attacks. *IEEE Trans Syst Man Cybern Syst*. 2019;49(8):1554-1569.
30. Zha L, Liu J, Cao J. Resilient event-triggered consensus control for nonlinear muti-agent systems with DoS attacks. *J Franklin Inst*. 2019;356(13):7071-7090.
31. De Persis C, Tesi P. Input-to-state stabilizing control under denial-of-service. *IEEE Trans Autom Control*. 2015;60(11):2930-2944.
32. Liu J, Wei L, Xie X, Yue D. Distributed event-triggered state estimators design for sensor networked systems with deception attacks. *IET Control Theory Appl*. 2019;13(17):2783-2791.
33. Du D, Zhang C, Wang H, Li X, Hu H, Yang T. Stability analysis of token-based wireless networked control systems under deception attacks. *Inform Sci*. 2018;459:168-182.
34. Ye D, Zhang T-Y. Summation detector for false data-injection attack in cyber-physical systems. *IEEE Trans Cybern*. 2020;50(6):2338-2345.
35. Ma L, Wang Z, Han Q-L, Lam H-K. Variance-constrained distributed filtering for time-varying systems with multiplicative noises and deception attacks over sensor networks. *IEEE Sensors J*. 2017;17(7):2338-2345.
36. Yang W, Lei L, Yang C. Event-based distributed state estimation under deception attack. *Neurocomputing*. 2017;270:145-151.
37. Gu Z, Zhou X, Zhang T, Yang F, Shen M. Event-triggered filter design for nonlinear cyber-physical systems subject to deception attacks. *ISA Trans*. 2020;104:130-137.
38. Ding D, Wang Z, Ho DWC, Wei G. Distributed recursive filtering for stochastic systems under uniform quantizations and deception attacks through sensor networks. *Automatica*. 2017;78:231-240.
39. Yue D, Fang J, Won S. Delay-dependent robust stability of stochastic uncertain systems with time delay and Markovian jump parameters. *Circuits Syst Signal Process*. 2003;22(4):351-365.
40. Peng C, Han Q-L, Yue D. Communication-delay-distribution-dependent decentralized control for large-scale systems with IP-based communication networks. *IEEE Trans Control Syst Technol*. 2013;21(3):820-830.

41. Yang Y, Yue D, Xue Y. Decentralized adaptive neural output feedback control of a class of large-scale time-delay systems with input saturation. *J Franklin Inst Eng Appl Math*. 2015;352(5):2129-2151.
42. Wang D, Zhang N, Wang J, Wang W. Cooperative containment control of multiagent systems based on follower observers with time delay. *IEEE Trans Syst Man Cybern Syst*. 2017;47(1):13-23.
43. Wang D, Wang D, Wang W. Necessary and sufficient conditions for containment control of multi-agent systems with time delay. *Automatica*. 2019;103:418-423.
44. Sun X, Gu Z, Yang F, Yan S. Memory-event-trigger-based secure control of cloud-aided active suspension systems against deception attacks. *Inform Sci*. 2020;543:1-17.
45. Gu Z, Fei S, Zhao Y, Tian E. Robust control of automotive active seat-suspension system subject to actuator saturation. *J Dyn Syst Measure Control*. 2014;136(4):041022.

How to cite this article: Sun X, Gu Z, Mu X. Observer-based memory-event-triggered controller design for quarter-vehicle suspension systems subject to deception attacks. *Int J Robust Nonlinear Control*. 2023;33(12):7004-7019. doi: 10.1002/rnc.6738